``Enseigner la recherche en train de se faire''

Chaire de
Physique de la Matière Condensée

THERMOELECTRICITE: CONCEPTS, MATERIAUX ET ENJEUX ENERGETIQUES

Antoine Georges

Cycle 2012-2013

Cours 4 – 17 avril 2013

- Thermopower and Entropy (cont'd)
- Thermodynamics of thermoelectrics; Efficiency (cont'd)
- Kubo formula for Onsager coefficients

Séminaire – 17 avril 2013

- Séminaire : 11h15 –

Franck GASCOIN, CRISMAT, Caen

Intermétalliques thermoélectriques d'hier, d'aujourd'hui... et de demain

Excerpt from abstract:

The aim of this seminar is to briefly describe the ideal criteria that must be met by thermoelectric materials and to show that with today's available innovative techniques of synthesis and analysis, new materials are found (antimonides, tellurides, selenides and even sulfides) and "ancient" materials (Bi_2Te_3, PbTe, SiGe) are improved.

1. Thermopower and Entropy (continued from lecture 3)

The Heikes and Shastry-Kelvin approximations to the thermoelectric power

$$\alpha_H = \frac{\mu}{eT} = -\frac{1}{e}\frac{\partial S}{\partial n}|_E$$

$$\alpha_{SK} = \frac{1}{e}\frac{\partial \mu}{\partial T}|_n = -\frac{1}{e}\frac{\partial S}{\partial n}|_T$$

Key point: why transition-metal compounds (e.g. oxides) may be good ?

→ Benefit from the large number of degrees of freedom
- hence large entropy -
(spin, orbitals: 10-fold in a d-shell)

- These degrees of freedom ar fully quenched
in the metallic regime for T<T*

- They get gradually unquenched at higher-T when
Electrons can be considered more localized
(→ Relevance of Heikes estimates in this regime)

- Frustration helps

Heikes, multi-orbital:

Hi-T (T>U):

$$\alpha_H = -\frac{k_B}{e} \ln \frac{2M-n}{n}$$

T<U, integer filling N

$$\alpha = \frac{k_B}{e} \ln \left[\frac{d_N}{d_{N+1}} \frac{n-N}{N+1-n} \right]$$

T<U, mixed valence N<n<N+1

$$\alpha = \frac{k_B}{e} \frac{1}{2} \ln \frac{d_{N-1}}{d_{N+1}}$$

case	degeneracies ; $\alpha[k_B/e]$ for $T < J < U$	$J < T < U$
$n = 1$	1,9 ; $-\log[9]/2$	1,15 ; $-\log[15]/2$
$n = 2$	6,4 ; $\log[3/2]/2$	6,20 ; $-\log[10/3]/2$
$n = 3$	9,9; 0	15,15; 0
$0 < n < 1$	1,6 ; $-\log[(1-x)/x] - \log 6$;	1,6; $-\log[(1-x)/x] - \log 6$
$1 < n < 2$	6,9 ; $-\log[(1-x)/x] - \log 3/2$	6,15; $-\log[(1-x)/x] - \log 5/2$
$2 < n < 3$	9,4 ; $-\log[(1-x)/x] - \log 4/9$	15,20 $-\log[(1-x)/x] - \log 4/3$
$U < T$	$\log[\frac{2M-n}{n}]$	

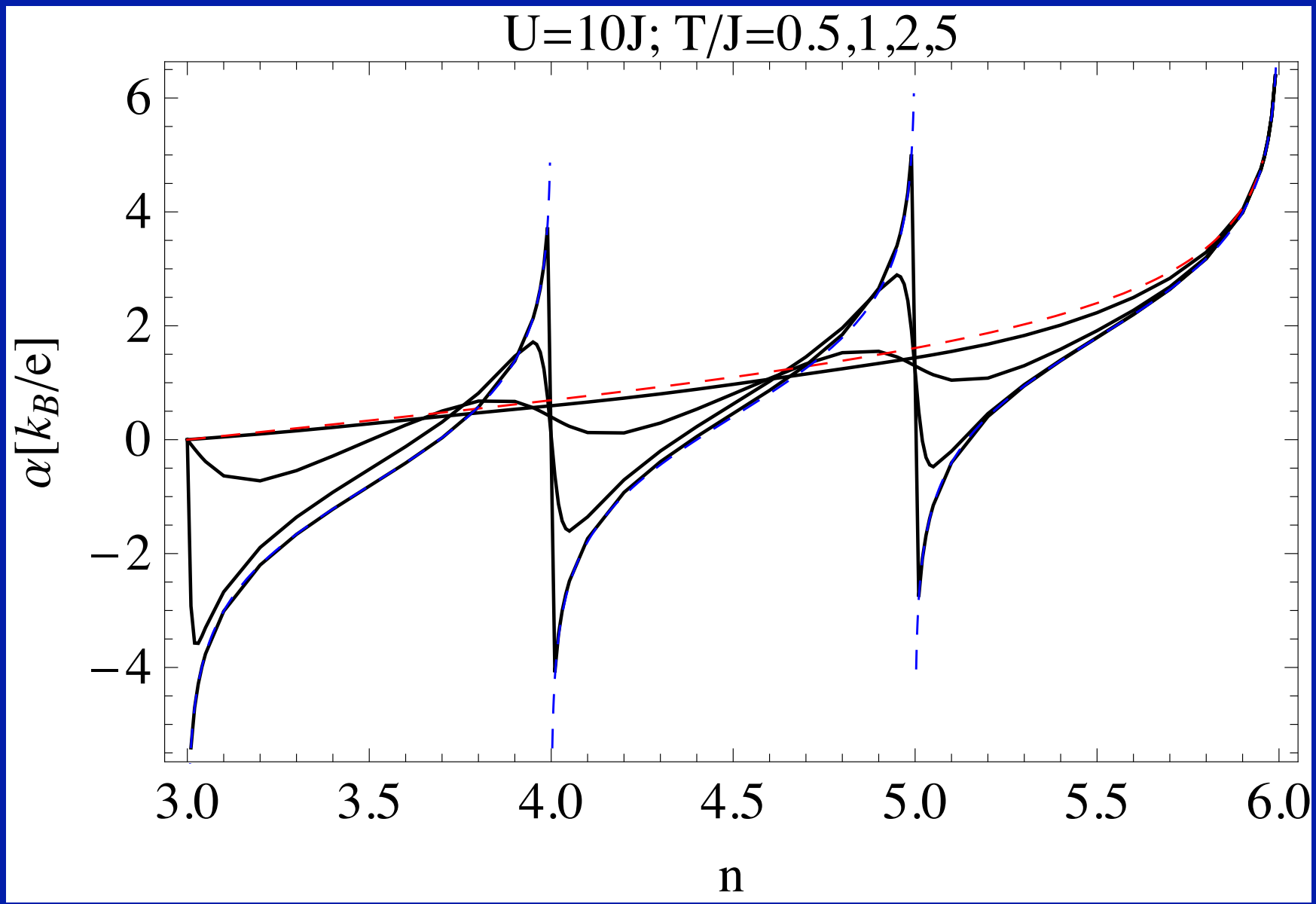

To visualize spin/orbital entropic contribution, look at filling N+1/2 in each case where the Heikes factor ln[x/(1-x)]=0

Semi-conducting oxides
for which
Heikes analysis
works

Heikes formula with spin and orbital degeneracy

$$S = \frac{-k_B}{|e|}\ln\left(\frac{1-x}{x}\right) + \frac{k_B}{|e|}\ln(\Gamma_{orb}\Gamma_{spin})$$

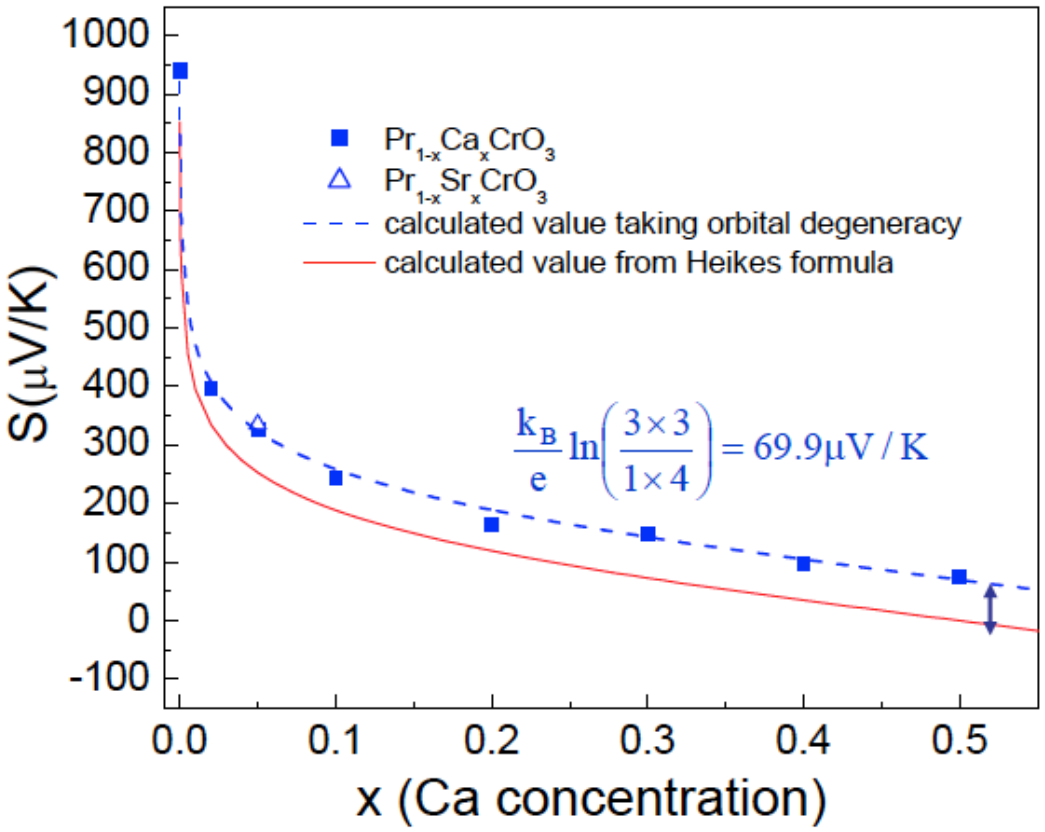

$3d^3$ $\Gamma_{orb}=1$ $\Gamma_{spin}=4$

$3d^2$ $\Gamma_{orb}=3$ $\Gamma_{spin}=3$

Marsh and Parris, Phys. Rev. B 54, 7720 (1996)

A case where Heikes works qualitatively, but not quantitatively: $La/SrVO_3$ [d^2/d^1]

PHYSICAL REVIEW B **83**, 165127 (2011)

Thermoelectric response in the incoherent transport region near Mott transition: The case study of $La_{1-x}Sr_xVO_3$

M. Uchida,[1] K. Oishi,[1] M. Matsuo,[2,3] W. Koshibae,[4] Y. Onose,[1,5] M. Mori,[2,3] J. Fujioka,[5] S. Miyasaka,[6] S. Maekawa,[2,3] and Y. Tokura[1,4,5]

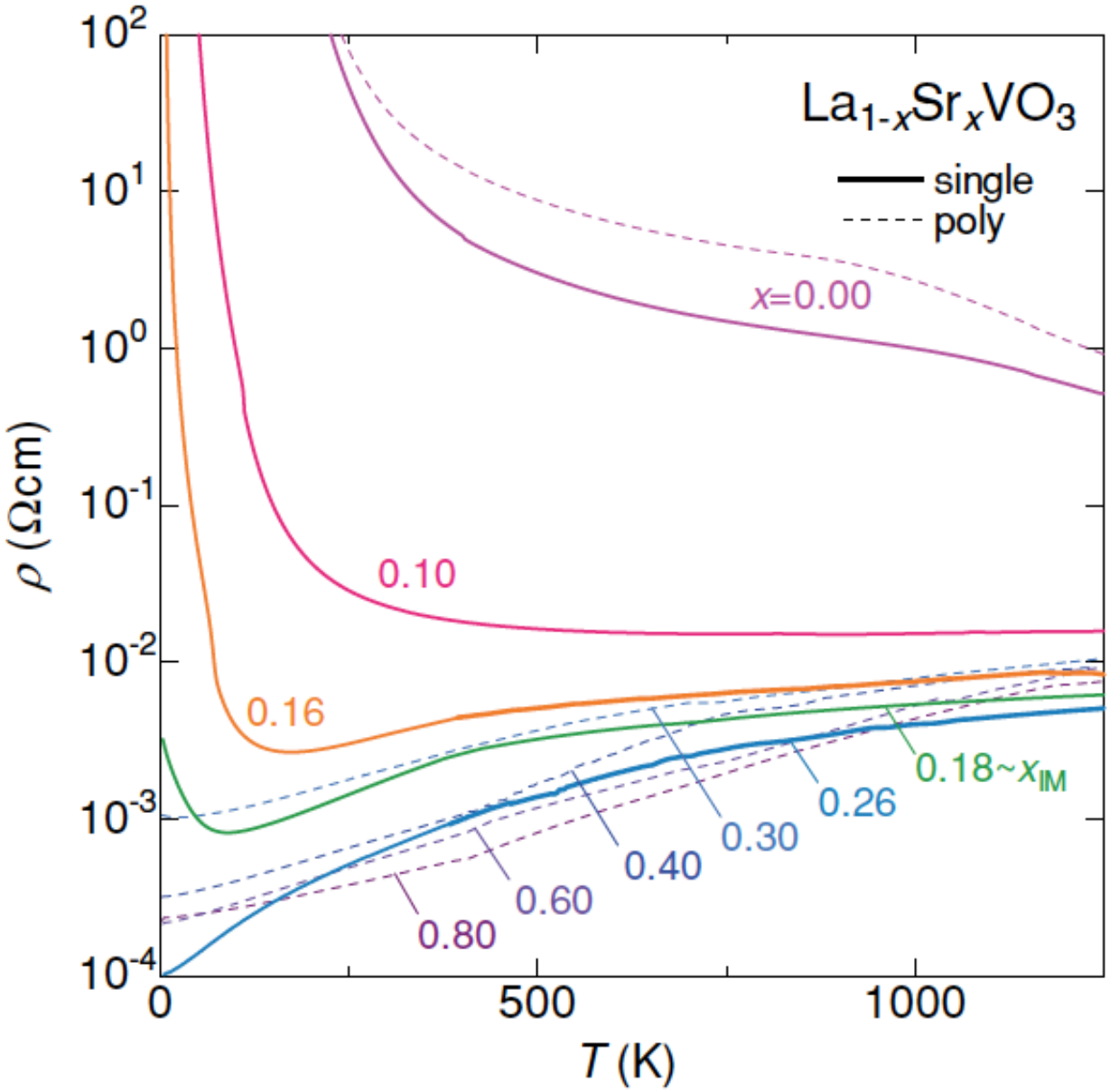

FIG. 1. (Color online). Temperature dependence of the resistivity ρ in $La_{1-x}Sr_xVO_3$. The solid and dashed lines represent the data for the single crystals and polycrystals, respectively.

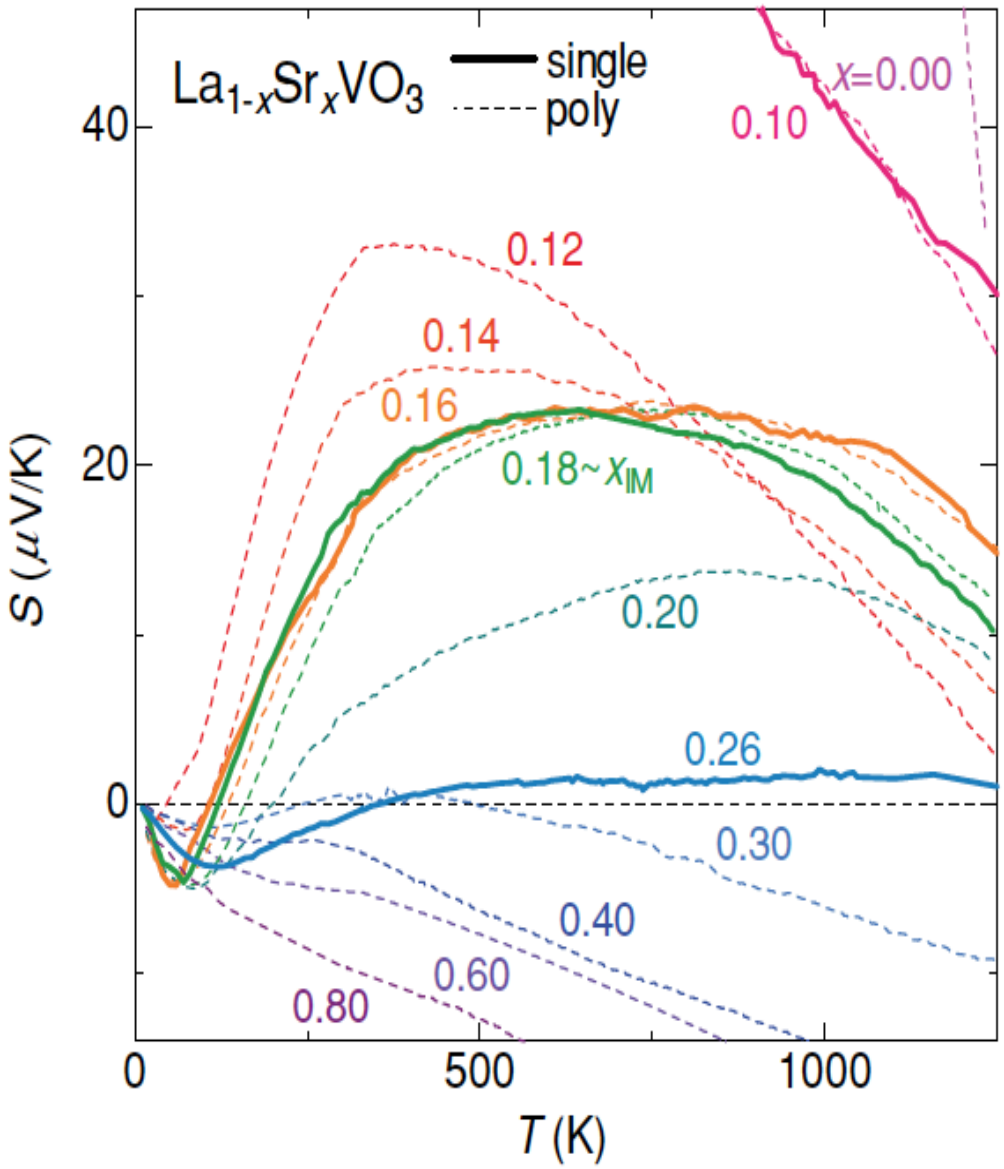

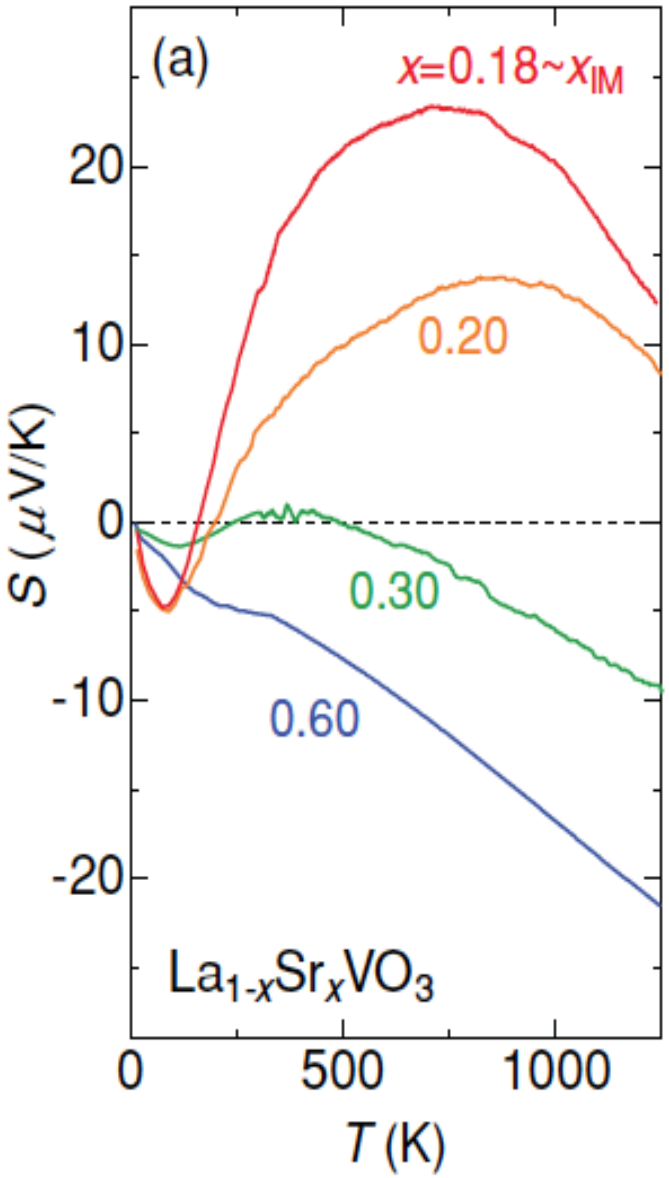

FIG. 3. (Color online). Temperature dependence of the thermopower S in $La_{1-x}Sr_xVO_3$. The solid and dashed lines represent the data for the single crystals and polycrystals, respectively.

Qualitatively quite similar to Hubbard model calculations above

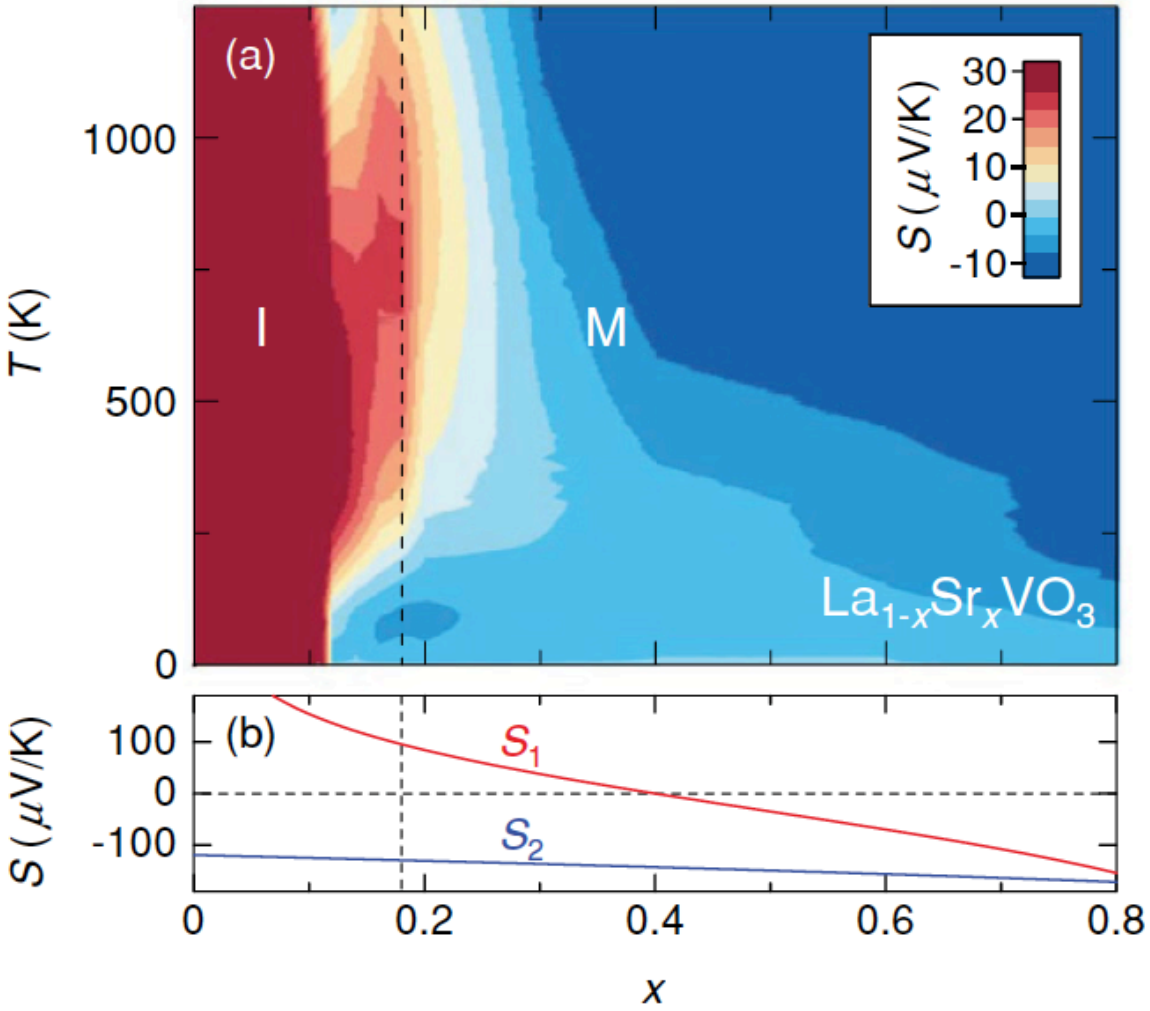

FIG. 4. (Color online). (a) Evolution of the thermopower S in the T-x phase diagram. The vertical dashed lines indicate the critical doping level x_{IM} for the insulator (I)-metal (M) transition at the ground state. The region with large S-gradient around x_{IM} corresponds to the incoherent metallic state as expected for the Heikes formula to be valid. (b) Doping variation of S in two high-temperature limits S_1 ($k_{\mathrm{B}}T \ll U$) and S_2 ($U \ll k_{\mathrm{B}}T$) in the Heikes formula with consideration of nearly degenerate t_{2g} or (t_{2g} plus e_g) orbitals (see text).

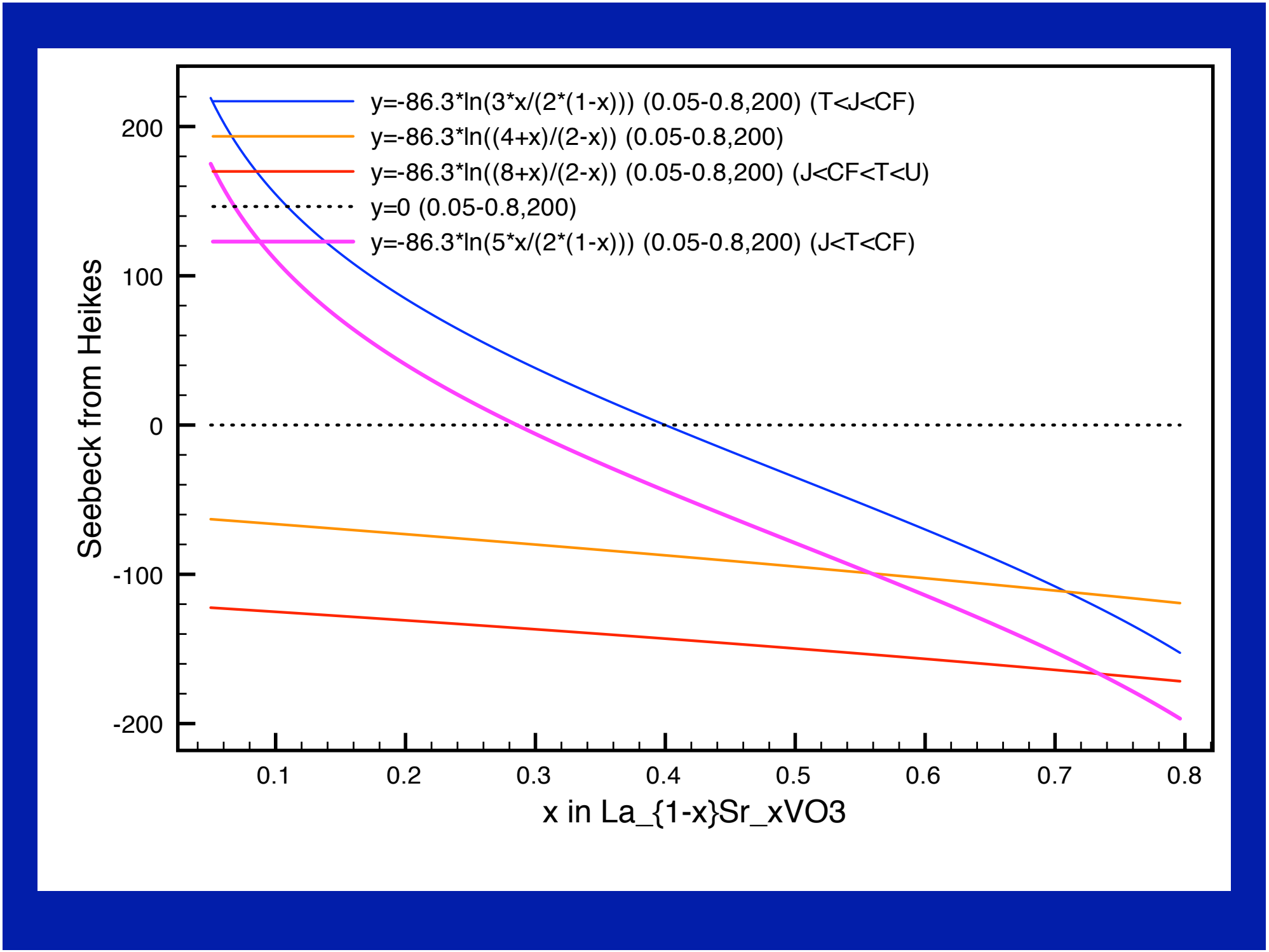
y=-86.3*ln(3*x/(2*(1-x))) (0.05-0.8,200) (T<J<CF)
y=-86.3*ln((4+x)/(2-x)) (0.05-0.8,200)
y=-86.3*ln((8+x)/(2-x)) (0.05-0.8,200) (J<CF<T<U)
y=0 (0.05-0.8,200)
y=-86.3*ln(5*x/(2*(1-x))) (0.05-0.8,200) (J<T<CF)
Seebeck from Heikes
200
100
0
-100
-200
0.1
0.2
0.3
0.4
0.5
0.6
0.7
0.8
x in La_{1-x}Sr_xVO3

Thermopower and Entropy: Cuprates

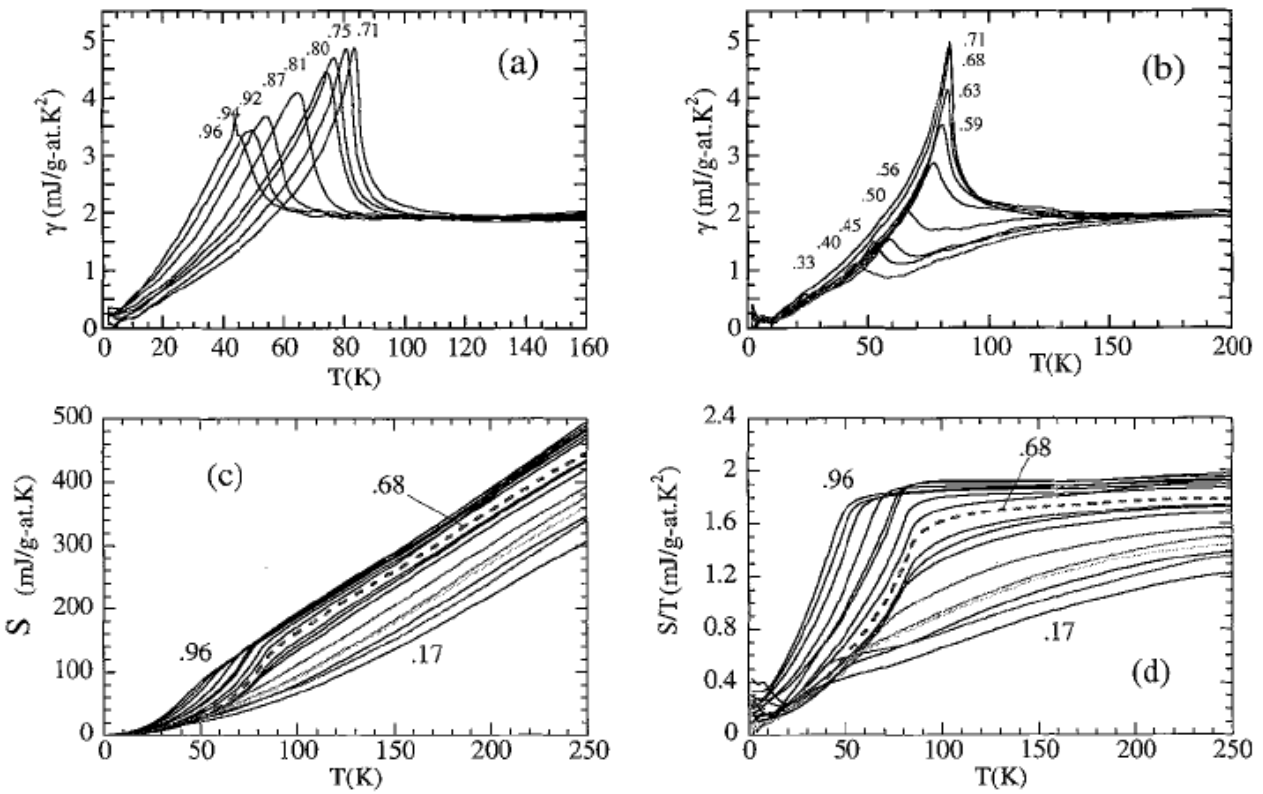

Fig. 2. The temperature dependence of the electronic specific heat coefficient γ(a) and (b), the electronic entropy S(c), and S/T(d), for $Y_{0.8}Ca_{0.2}Ba_2Cu_3O_{6+x}$ with x ranging from 0.96 to 0.17.

Loram, Cooper et al.

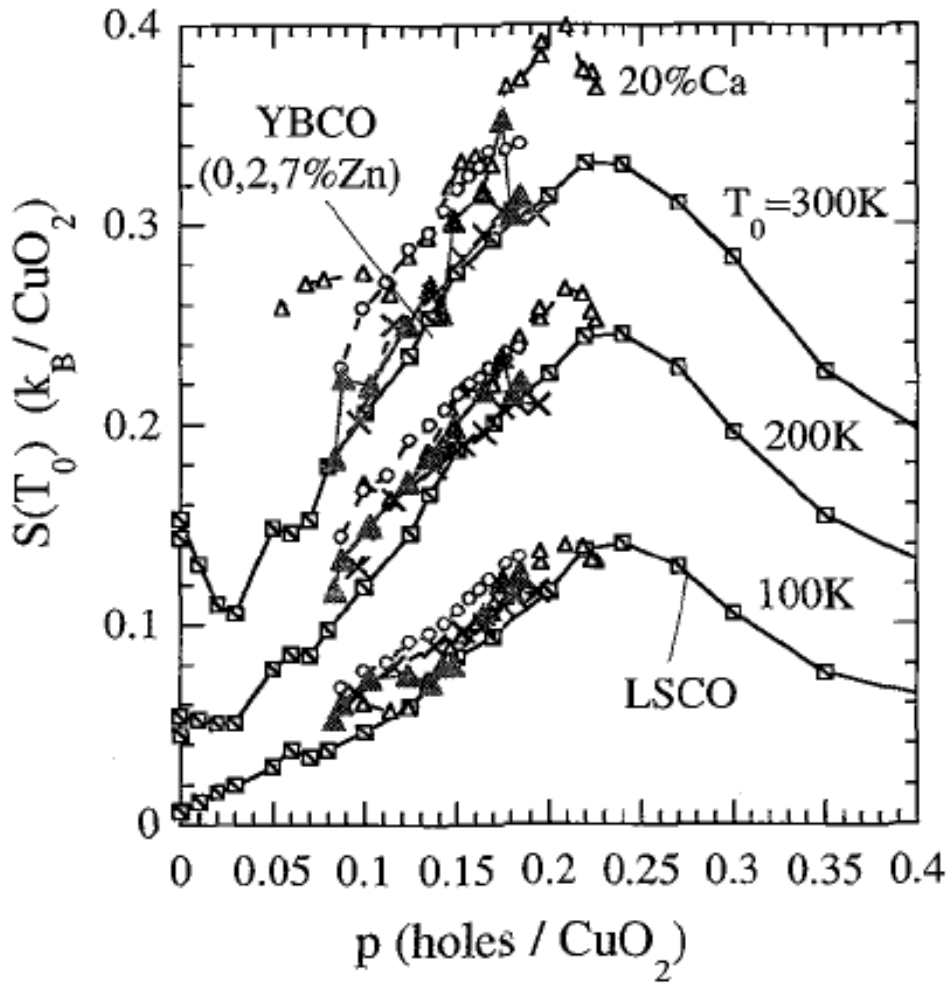

Fig. 3. Electronic entropy $S(T_0)$ (in units of k_B/CuO_2) *vs.* p for three fixed temperatures (T_0). Crossed squares $La_{2-x}Sr_xCuO_4$, closed triangles $YBCO_{6+x}$, circles $YBCO_{6+x}$(0.02Zn), crosses $YBCO_{6+x}$(0.07Zn), and open triangles $YBCO_{6+x}$(0.2Ca).

Obertelli, Cooper, Tallon PRB 46 R14928 (1992)

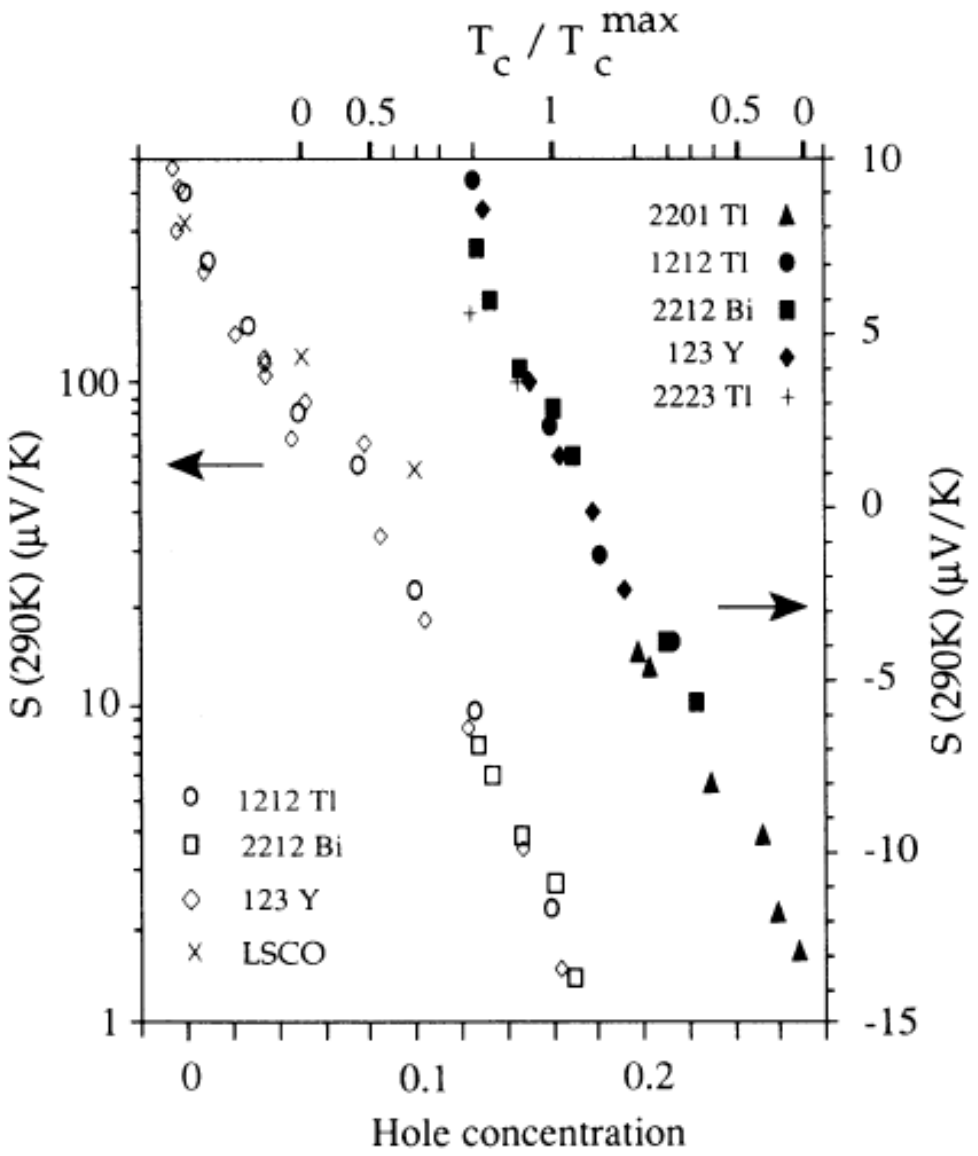

FIG. 3. Room-temperature thermoelectric power $S(290\ \mathrm{K})$ vs hole concentration (and T_c/T_c^{max}) for various high-T_c cuprates in both the underdoped (logarithmic scale) and overdoped (linear scale) regions. $La_{2-x}Sr_xCuO_4$ (LSCO) data from Ref. 33.

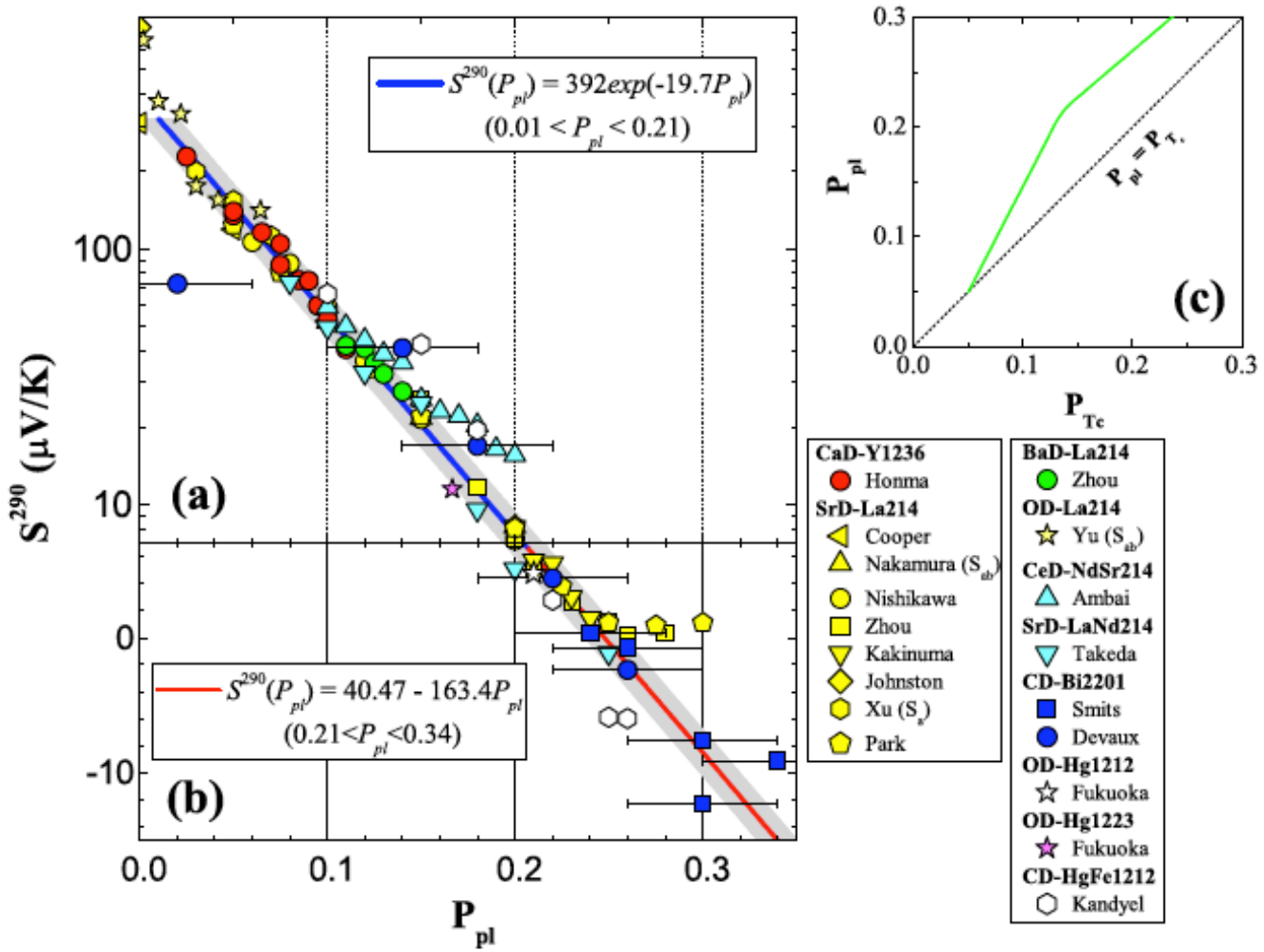

FIG. 2. (Color online) S^{290} as a function of the hole-doping content per CuO_2 plane. (a) S^{290} (≥ 7 μV/K) on the upper panel is plotted on a logarithmic scale, while (b) S^{290} (<7 μV/K) on the lower panel is plotted on a linear scale. The plotted data are summarized in Table IV. (c) Quantitative comparison between P_{pl} and P_{T_c}. The dotted line shows $P_{pl}=P_{T_c}$. We used this relation for the conversion from P_{T_c} into P_{pl}. The error of P_{pl} is below 0.04 for the CD-Bi2201 and below 0.01 for all other HTSs. The error bar for the other materials is not shown. The shaded area represents a region with the P_{pl} error of ± 0.01 around the universal $S^{290}(P_{pl})$ curve.

Honma and Hor PRB 2008

2. EFFICIENCY OF ENERGY CONVERSION

Application to thermoelectrics

(continued from lecture 2…)

Maximum theoretical efficiency: the Carnot reversible engine

Carnot efficiency:

$$\eta_C = 1 - \frac{T_C}{T_H}$$

Since it corresponds to a reversible, quasi-static and hence infinitely slow process, a Carnot engine delivers ZERO POWER !

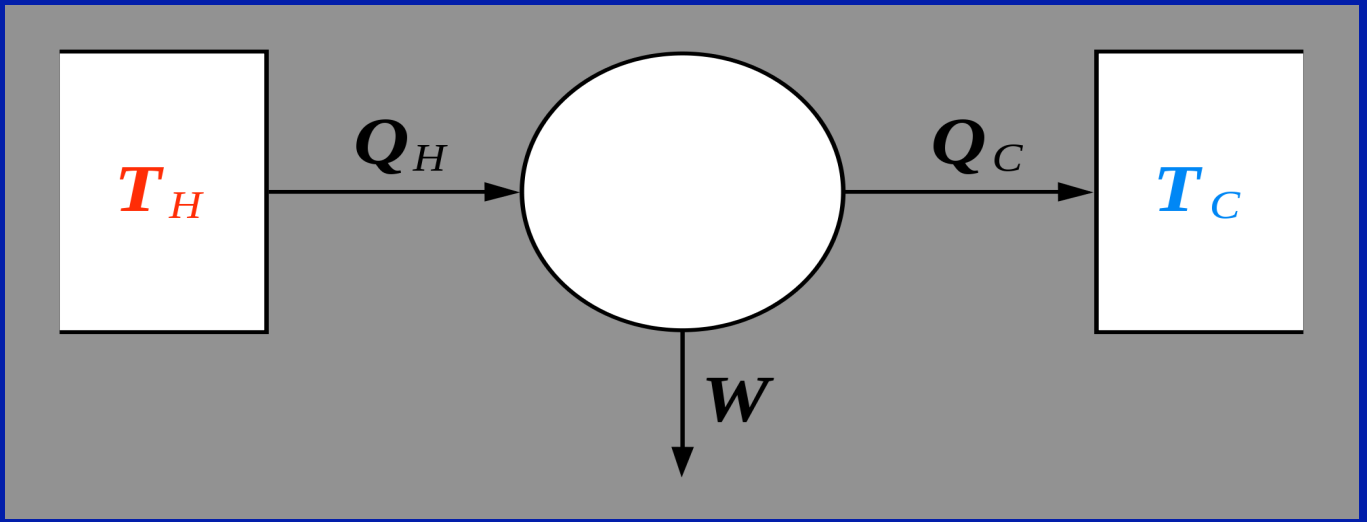

Carnot cycle :

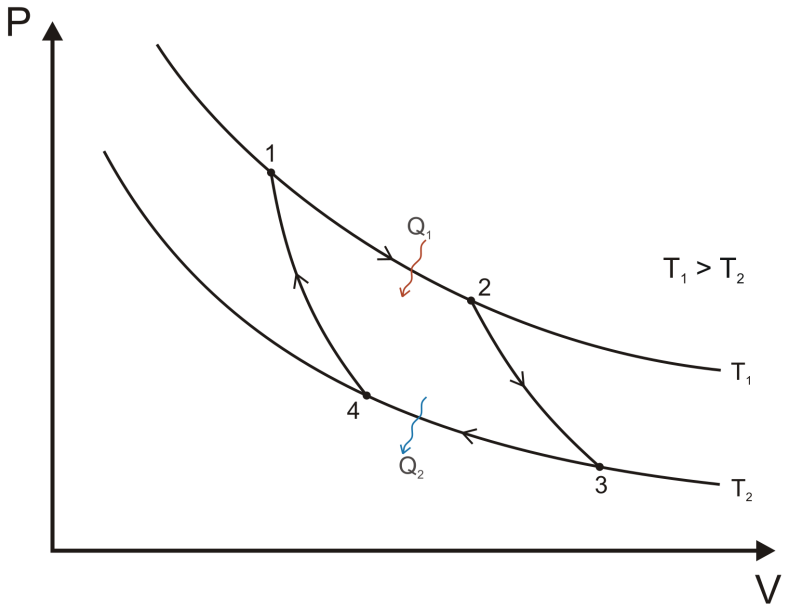

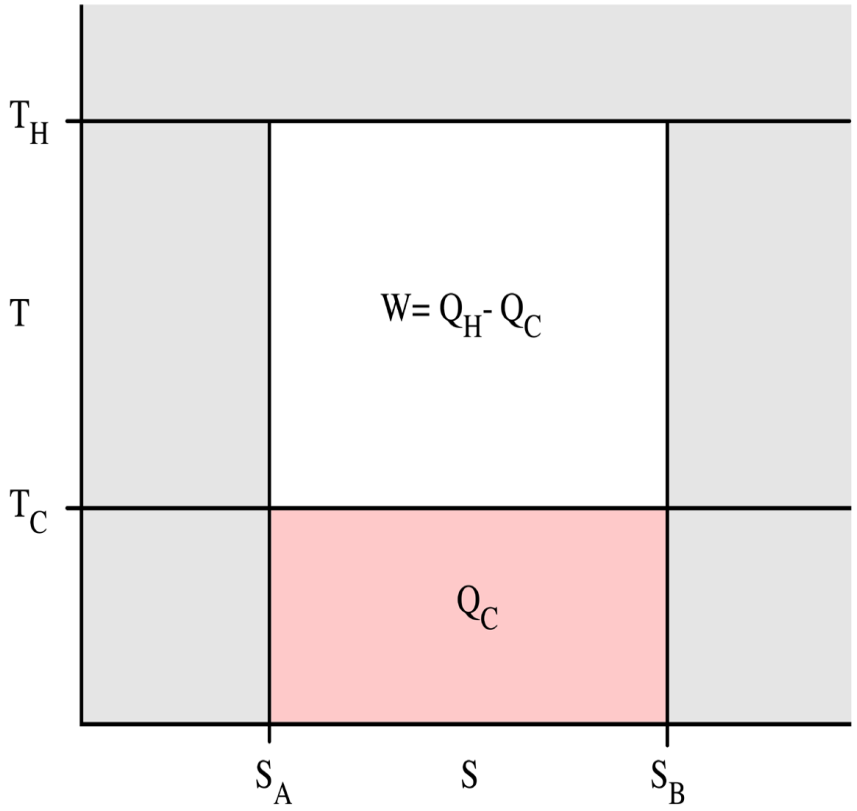

Efficiency at maximum power,

according to:

Chambadal-Novikov

(Curzon-Ahlborn),

Endoreversible engines,

« Finite-Time Thermodynamics »

An endoreversible engine

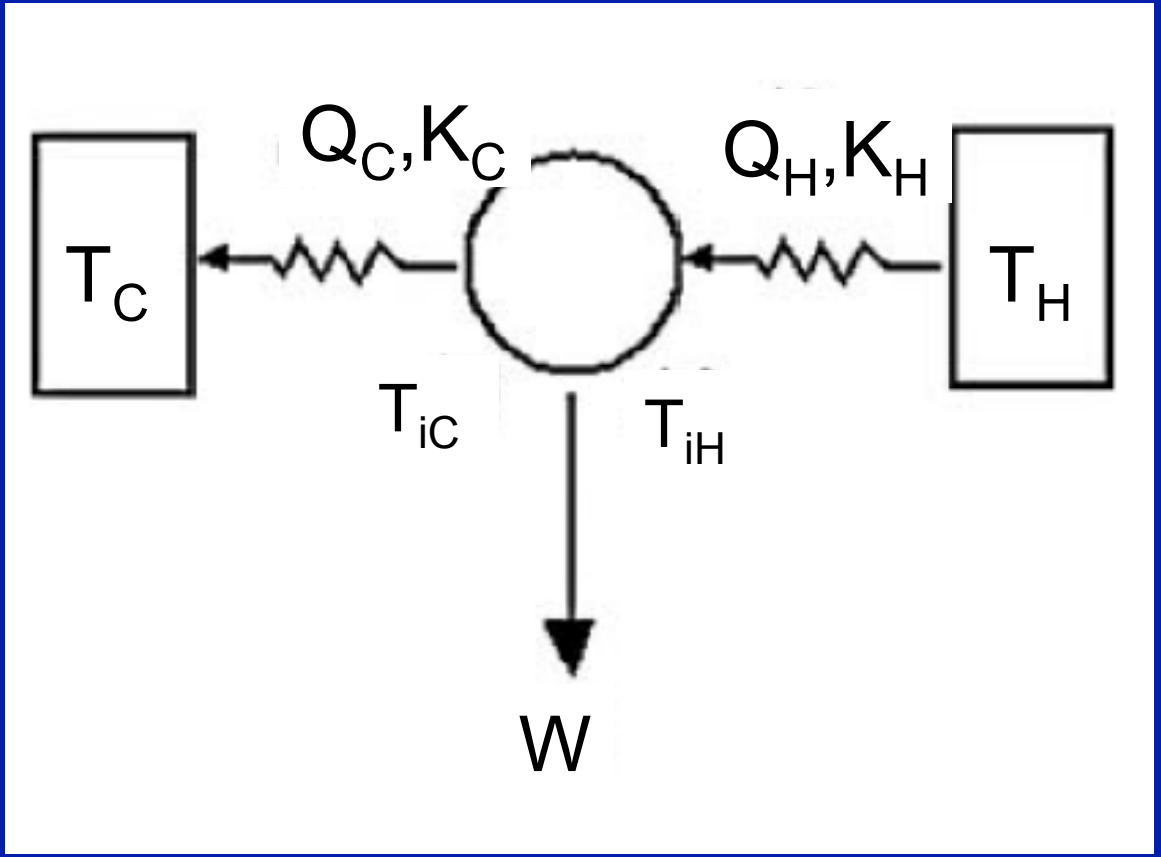

$$\eta(P_{\max}) = 1 - \sqrt{\frac{T_C}{T_H}}$$

Chambadal-Novikov Efficiency

½ of Carnot for small ΔT

$$P_{\max} = \frac{K_H K_C}{(\sqrt{K_H} + \sqrt{K_C})^2} \left[\sqrt{T_H} - \sqrt{T_C}\right]^2$$

Key coupling constant characterizing energy conversion :

$$g \equiv \frac{L_{12}}{\sqrt{L_{11}L_{22}}} \ , \ g^2 = \frac{\overline{z}}{1+\overline{z}}$$

$$\det \underline{L} \geq 0 \quad \Rightarrow \quad -1 \leq g \leq +1$$

Entropy and heat production rates

$$T\left[\frac{\partial s}{\partial t}+\boldsymbol{\nabla}\cdot\boldsymbol{j}_s\right]=\boldsymbol{j}_s\cdot(-\boldsymbol{\nabla}T)+\boldsymbol{j}_n\cdot(-\boldsymbol{\nabla}\mu)$$

$$\frac{\partial s}{\partial t}|_{prod}\equiv\frac{\partial s}{\partial s}+\boldsymbol{\nabla}\cdot\boldsymbol{j}_s=\frac{1}{T}\boldsymbol{G}\cdot\underline{L}\boldsymbol{G}$$

$$\boldsymbol{G}\equiv\begin{pmatrix}-\boldsymbol{\nabla}\mu\\-\boldsymbol{\nabla}T\end{pmatrix}$$

$$\frac{\partial Q}{\partial t}|_{irr}\equiv\left[\frac{\partial s}{\partial t}+\boldsymbol{\nabla}\cdot\boldsymbol{j}_s\right]=\rho\boldsymbol{j}_e^2+\frac{\kappa}{T}(\boldsymbol{\nabla}T)^2$$

Entropy and heat production rates

$$T\left[\frac{\partial s}{\partial t}+\boldsymbol{\nabla}\cdot\boldsymbol{j}_s\right]=\boldsymbol{j}_s\cdot(-\boldsymbol{\nabla}T)+\boldsymbol{j}_n\cdot(-\boldsymbol{\nabla}\mu)$$

$$\frac{\partial s}{\partial t}|_{prod}\equiv\frac{\partial s}{\partial s}+\boldsymbol{\nabla}\cdot\boldsymbol{j}_s=\frac{1}{T}\boldsymbol{G}\cdot\underline{L}\boldsymbol{G}$$

$$\boldsymbol{G}\equiv\begin{pmatrix}-\boldsymbol{\nabla}\mu\\-\boldsymbol{\nabla}T\end{pmatrix}$$

$$\frac{\partial Q}{\partial t}|_{irr}\equiv\mathsf{T}\left[\frac{\partial s}{\partial t}+\boldsymbol{\nabla}\cdot\boldsymbol{j}_s\right]=\rho\boldsymbol{j}_e^2+\frac{\kappa}{T}(\boldsymbol{\nabla}T)^2$$

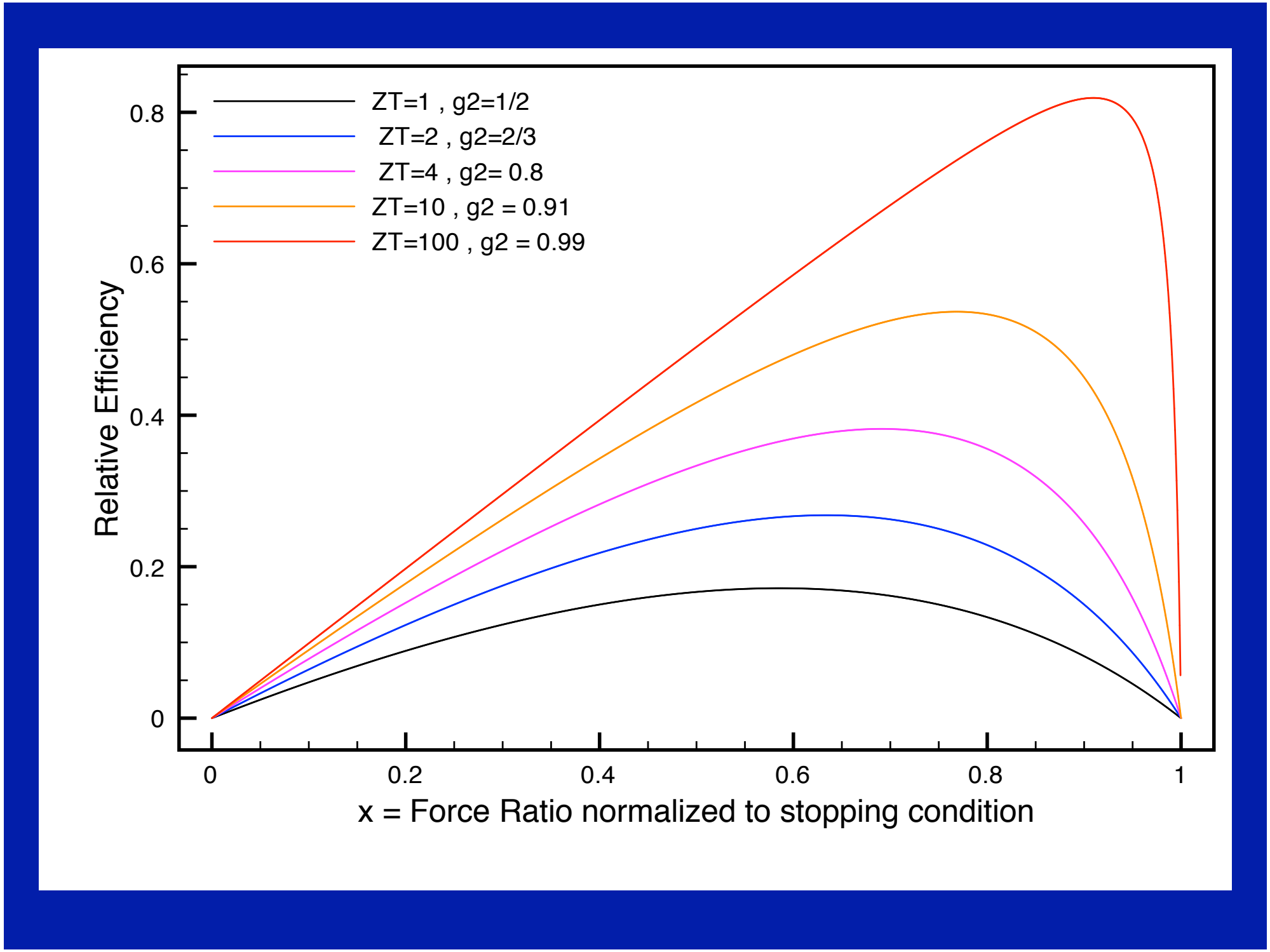
ZT=1 , g2=1/2
ZT=2 , g2=2/3
ZT=4 , g2= 0.8
ZT=10 , g2 = 0.91
ZT=100 , g2 = 0.99
Relative Efficiency
0
0.2
0.4
0.6
0.8
0
0.2
0.4
0.6
0.8
1
x = Force Ratio normalized to stopping condition

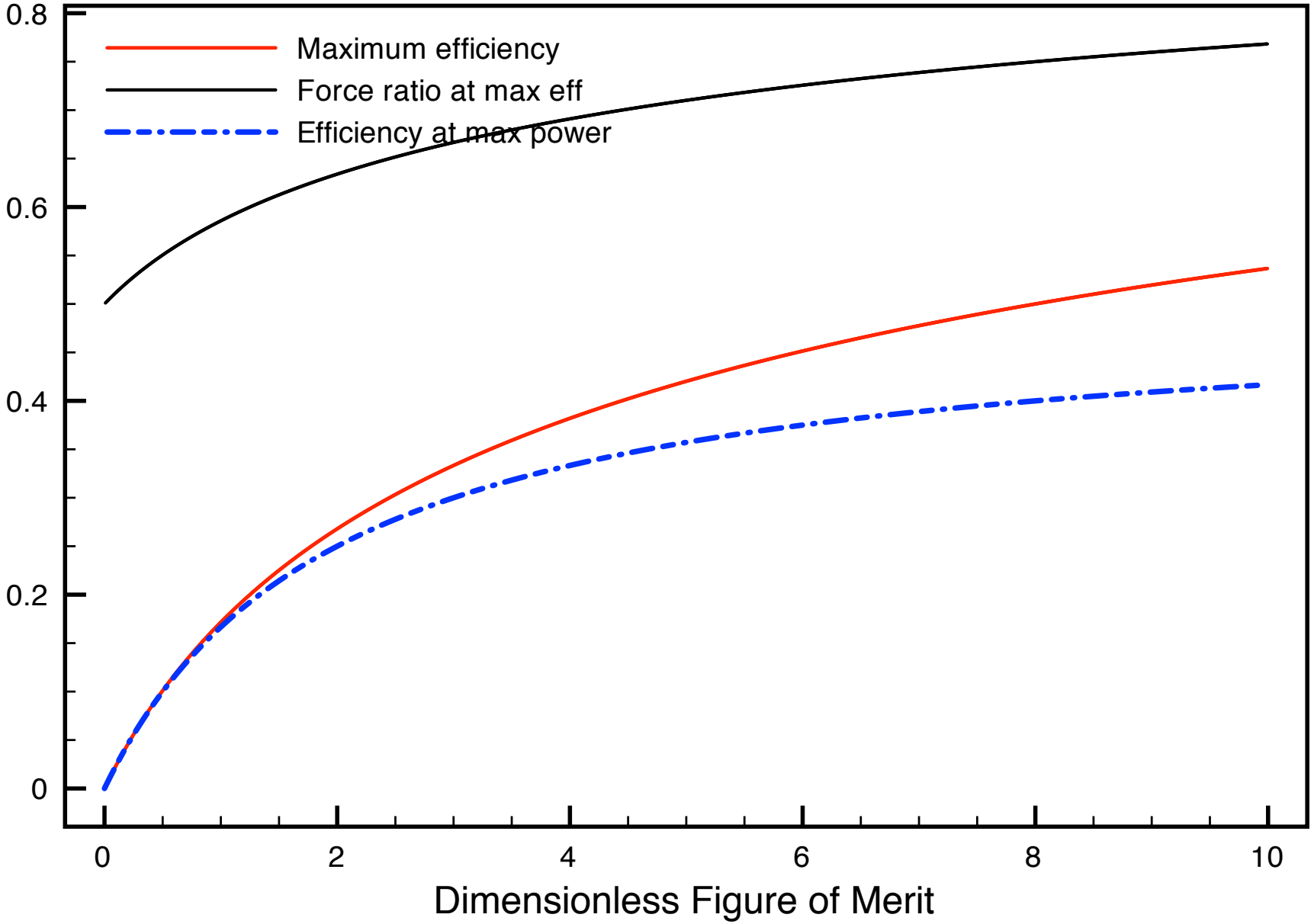
0.8
0.6
0.4
0.2
0
Maximum efficiency
Force ratio at max eff
Efficiency at max power
0
2
4
6
8
10
Dimensionless Figure of Merit

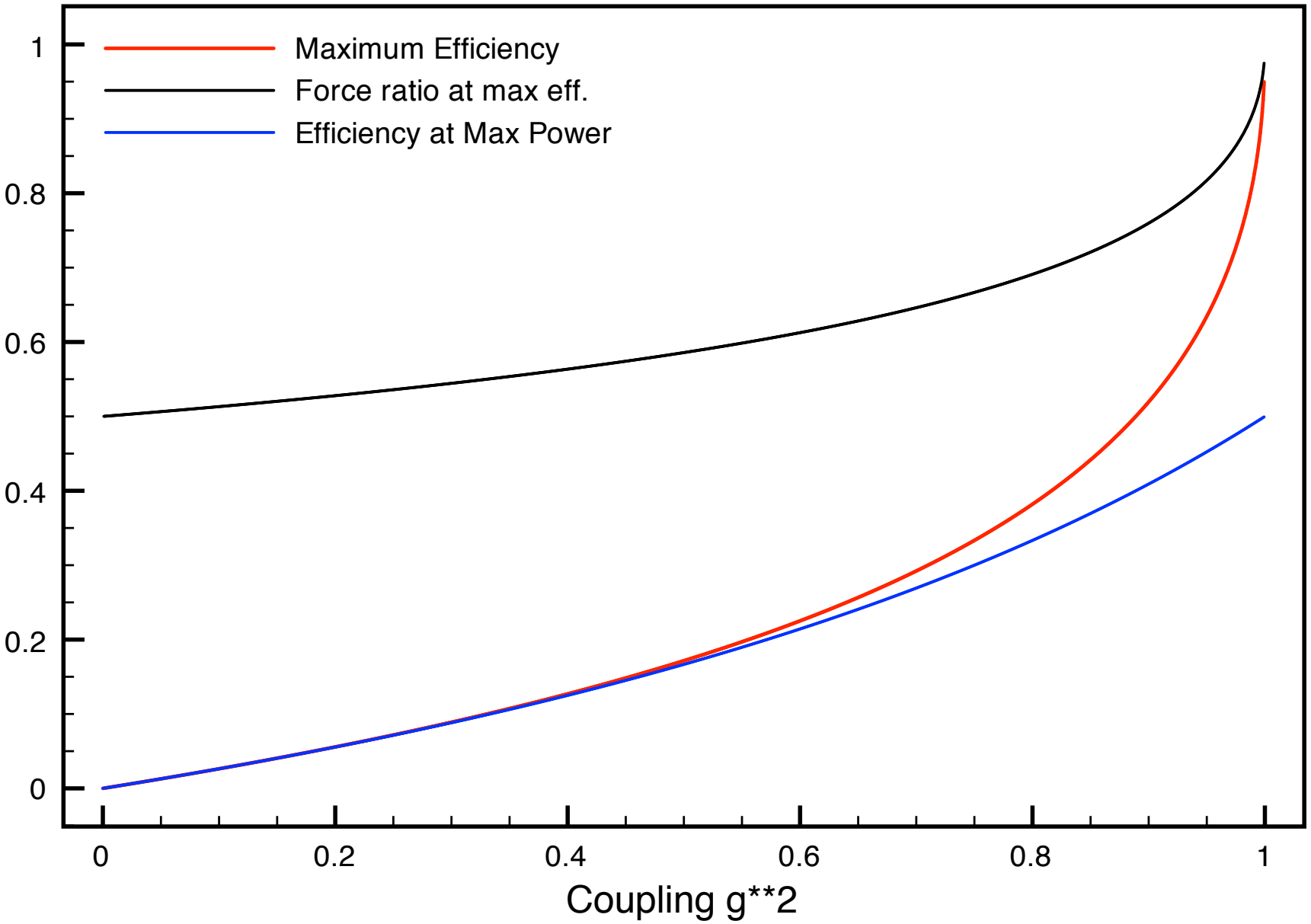
Maximum Efficiency
Force ratio at max eff.
Efficiency at Max Power
1
0.8
0.6
0.4
0.2
0
0
0.2
0.4
0.6
0.8
1
Coupling g**2

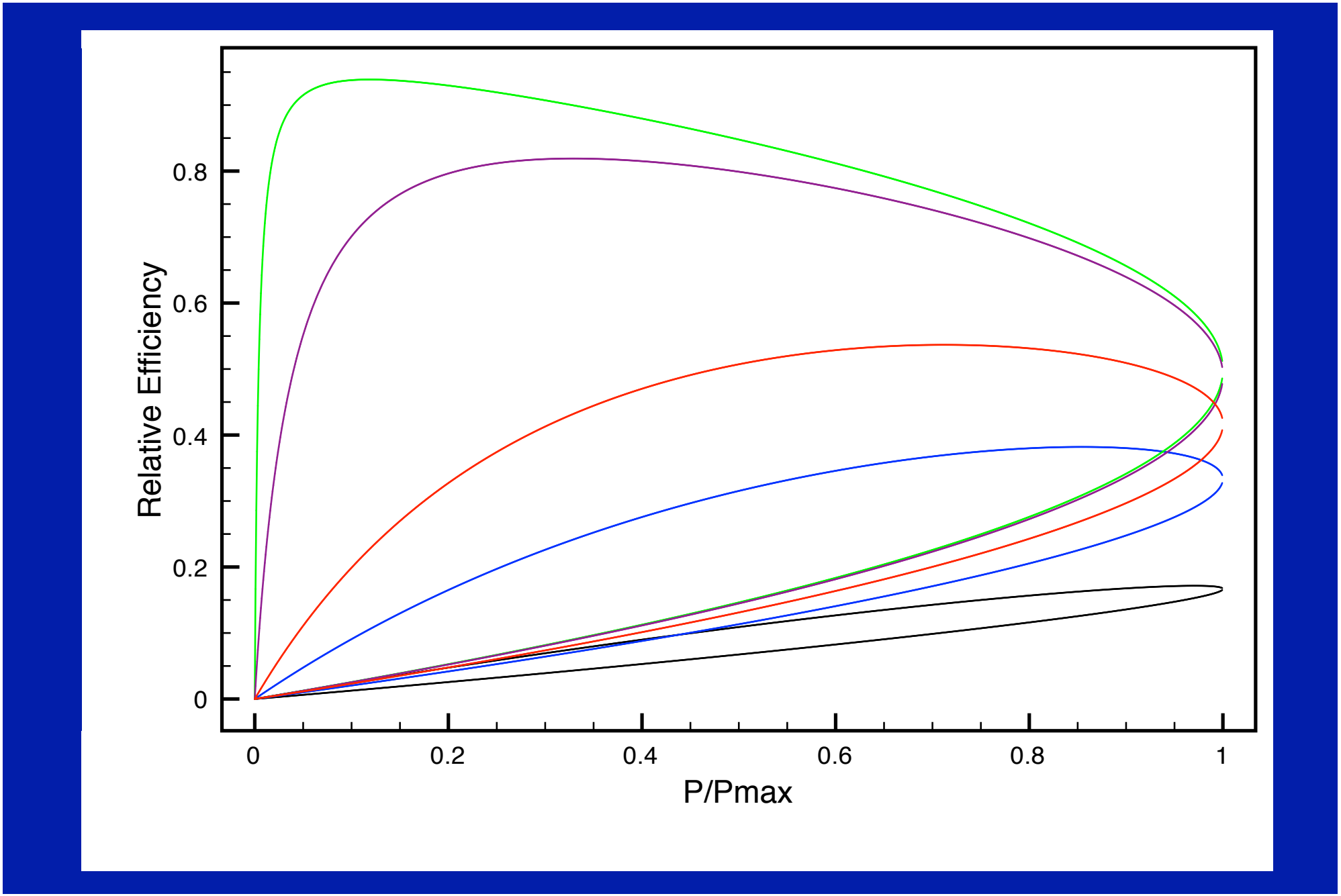

FIG. 4: Relative efficiency vs. power normalized to its maximum value, for (bottom to top): $\overline{z} = 1, 4, 10, 100, 1000$. The upper (resp. lower) branches correspond to a force ratio $x \geq 1/2$ (resp. $x \leq 1/2$). Maximum efficiency is realized on the upper branch.

3. Onsager coefficients from Kubo formula

- G.D. Mahan, Many-Particle Physics Sec. 3.8-3.9
- R. Kubo J.Phys Soc Jpn 12, 570 (1957)
- J.M. Luttinger Phys Rev 135, A1505 (1964)
- MR Peterson and BS Shastry PRB 82, 195105 (2010)
- Detailed derivation of simplifications in DMFT: Paul and Kotliar PRB 67, 115131 (2003)

I will skip most details, just emphasizing some key (and sometimes subtle…) points

Formal aspects only,
→ several concrete applications in lectures 5-6 next week

3.1 Kubo, electrical conductivity

- Linear response to a small perturbing field.
- Two strategies:
- a) Time- (and space-) dependent vector potential to generate electric field: $\sigma(q,\omega)$
- b) Gradient of scalar potential (Luttinger)
  → Caution: dont want to just generate a carrier-density profile which adapts to potential, want to generate current
  → Branch on potential in an adiabatic, time - dependent manner

Result of first approach:

$$\sigma_{\alpha\beta}(\mathbf{q},\omega) = \frac{1}{\omega\nu}\int_{-\infty}^{t} dt' e^{i\omega(t-t')}\langle\psi|[j_\alpha^\dagger(\mathbf{q},t), j_\beta(\mathbf{q},t')]|\psi\rangle + i\frac{n_0 e^2}{m\omega}\delta_{\alpha\beta}$$

Conductivity is related to the retarded current-current correlation function

$$\Pi_{\alpha\beta}(\mathbf{q},\omega) = -\frac{i}{\nu}\int_{-\infty}^{\infty} dt e^{i\omega(t-t')}\Theta(t-t')\langle\psi|[j_\alpha^\dagger(\mathbf{q},t), j_\beta(\mathbf{q},t')]|\psi\rangle$$

$$\sigma_{\alpha\beta}(\mathbf{q},\omega) = \frac{i}{\omega}\left[\Pi_{\alpha\beta}(\mathbf{q},\omega) + \frac{n_0 e^2}{m}\delta_{\alpha\beta}\right]$$

Fast limit: first take q → 0, THEN ω → 0
Spectral (Lehmann) representation:

$$-\mathrm{Im}[\Pi_{\alpha\beta}(\omega)] = \tfrac{1}{2} R_{\alpha\beta}(\omega)$$
$$= \frac{\pi}{\nu}(1 - e^{-\beta\omega}) e^{\beta\Omega} \sum_{nm} e^{-\beta E_N} \langle n | j_a^\dagger | m \rangle \langle m | j_\beta | n \rangle$$
$$\times \delta(\omega + E_n - E_m) \qquad (3.394)$$

Now it is straightforward to take the limit $\omega \to 0$, since the prefactor of the above equation is

$$\lim_{\omega \to 0} \frac{1}{\omega}(1 - e^{-\beta\omega}) = \beta \qquad (3.395)$$

and

$$\mathrm{Re}(\sigma_{\alpha\beta}) = \frac{\pi\beta}{\nu} \sum_{nm} e^{-\beta E_n} \langle n | j_\beta | m \rangle \langle m | j_\alpha | n \rangle \delta(E_n - E_m)$$

The conductivity is finite as $\omega \to 0$. There is no divergence in this limit, even though there is the ω^{-1} factor in (3.393).

Second approach, for static (ω=0) conductivity: introduce adiabatically a scalar potential

$$e^{st} \int d^3 r \phi(\vec{r}) \rho(\vec{r})$$ s: small; q→0 first, then s→0

$$\mathrm{Re}\sigma_{\alpha\beta} = \frac{1}{V} \int_0^\infty dt e^{-st} \int_0^\beta d\tau \, \mathrm{Tr} \left[\hat{\rho}_0 \int d^3 r j_\beta(\vec{r}, -t - i\tau) j_\alpha(\vec{0}, 0) \right]$$

Mixes real and imaginary time; extra integration

From spectral representation, one can show that this expression Is actually identical to the previous one

Perturbing term in Hamiltonian: $e^{st}F$

$$F = \int d^3r\, \phi(r)\, \rho(r,t)$$

$$\frac{\partial F}{\partial t} = \int d^3r\, \phi(r)\, \frac{\partial \rho}{\partial t} = -\int d^3r \phi(r)\, \nabla j$$

$$= -\int d^3r \vec{E} \cdot \vec{j_e}$$

$$\langle j_A \rangle = -\int_0^\infty dt e^{-st} \int_0^\beta d\tau\, \mathrm{Tr}\left[\hat{\rho}_0\, \frac{\partial F(-t - i\tau)}{\partial t}\, j_A\right]$$

Currents and conjugate forces:

$$\frac{\partial S}{\partial t}|_{\rm irr} = \sum_A J_A . X_A$$

$$A = N, S \Rightarrow X_N = -\frac{1}{T}\nabla\mu \ , \ X_S = -\frac{1}{T}\nabla T$$

Linear response: $J_A = \sum_B L_{AB} X_B$

$$L_{AB} = -\frac{1}{\beta}\int_0^\infty dt e^{-st}\int_0^\beta d\tau \, {\rm Tr}\left[\hat{\rho}_0 \, j_A(-t - i\tau) j_B(0)\right]$$

$$L_{AB} = \pi \sum_{nm} e^{-\beta E_n} \langle n|j_A|m\rangle \langle m|j_B|n\rangle \, \delta(E_n - E_m)$$

Onsager symmetry is manifest on this form